Biol Blood Marrow Transplant 25 (2019) 2338–2349

Biology of Blood and Marrow Transplantation

journal homepage: www.bbmt.org

Biology

Modeling Chronic Graft-versus-Host Disease in MHC-Matched Mouse Strains: Genetics, Graft Composition, and Tissue Targets

Antonia M.S. Müller[1,2,*], Dullei Min[3], Gerlinde Wernig[4], Robert B. Levy[5], Victor L. Perez[6], Samantha Herretes[6], Mareike Florek[1], Casey Burnett[1], Kenneth Weinberg[2], Judith A. Shizuru[1,3]

[1] *Division of Blood and Marrow Transplantation, Department of Medicine, Stanford University School of Medicine, Stanford, California*
[2] *Department of Hematology, University Hospital and University Zurich, Zurich, Switzerland*
[3] *Division of Pediatric Blood and Marrow Transplantation, Stanford University School of Medicine, Stanford, California*
[4] *Department of Pathology, Stanford University School of Medicine, Stanford, California*
[5] *Department of Microbiology and Immunology, University of Miami Miller School of Medicine, Miami, Florida*
[6] *Department of Ophthalmology, University of Miami Miller School of Medicine, Miami, Florida*

Article history:
Received 10 November 2018
Received in revised from
22 June 2019
Accepted 6 August 2019

Keywords:
Mouse models
Chronic graft-versus-host disease
Pathophysiology
Thymic damage

A B S T R A C T

Graft-versus-host disease (GVHD) remains a major complication of allogeneic hematopoietic cell transplantation. Acute GVHD (aGVHD) results from direct damage by donor T cells, whereas the biology of chronic GVHD (cGVHD) with its autoimmune-like manifestations remains poorly understood, mainly because of the paucity of representative preclinical models. We examined over an extended time period 7 MHC-matched, minor antigen–mismatched mouse models for development of cGVHD. Development and manifestations of cGVHD were determined by a combination of MHC allele type and recipient strain, with BALB recipients being the most susceptible. The C57BL/6 into BALB.B combination most closely modeled the human syndrome. In this strain combination moderate aGVHD was observed and BALB.B survivors developed overt cGVHD at 6 to 12 months affecting eyes, skin, and liver. Naïve $CD4^+$ cells caused this syndrome as no significant pathology was induced by grafts composed of purified hematopoietic stem cells (HSCs) or HSC plus effector memory $CD4^+$ or $CD8^+$ cells. Furthermore, co-transferred naïve and effector memory $CD4^+$ T cells demonstrated differential homing patterns and locations of persistence. No clear association with donor Th17 cells and the phenotype of aGVHD or cGVHD was observed in this model. Donor $CD4^+$ cells caused injury to medullary thymic epithelial cells, a key population responsible for negative T cell selection, suggesting that impaired thymic selection was an underlying cause of the cGVHD syndrome. In conclusion, we report for the first time that the C57BL/6 into BALB.B combination is a representative model of cGVHD that evolves from immunologic events during the early post-transplant period.

INTRODUCTION

Chronic graft-versus-host disease (cGVHD) remains a major obstacle to the success of allogeneic hematopoietic cell transplantation (HCT) occurring in 30% to 70% of patients and contributing to 50% of late nonrelapse mortality. Historically, acute GVHD (aGVHD) and cGVHD were distinguished by their onset before and after day +100 post-HCT, respectively. However, for both human and mouse models this timing is not strictly representative. Hence, clinical features rather than the time relative to transplant are more commonly used to delineate the 2 syndromes [1,2].

In aGVHD the proinflammatory environment generated by the preparative conditioning together with infiltration of alloreactive donor T cells result in tissue damage, primarily affecting the intestines, skin, and liver [3]. The clinical spectrum and phenotypes of cGVHD are much broader and can manifest with or without preceding or overlapping features of aGVHD [1,2]. cGVHD typically involves fibrotic tissue transformation and often has features resembling autoimmune and other immunologic disorders [4-7]. The pathophysiology of cGVHD is complex, involving a mix of chronic inflammation, cell-mediated and humoral immunity, and fibrogenesis but, in general, is poorly understood.

For aGVHD preclinical mouse studies have been critical for elucidating the pathophysiology and guided development of an array of effective treatments. In contrast, for cGVHD corticosteroids remain the mainstay of treatment, and once disease becomes refractory to steroids, effective treatments are scarce. Although potential therapeutic targets have been identified in mouse models, none of these drug interventions has been successfully translated into clinical practice [8-11]. Rather, some

Financial disclosure: See Acknowledgments on page 2348.

* Correspondence and reprint requests: Antonia M. S. Müller, MD, Stanford University School of Medicine, Department of Medicine, Division of Blood and Marrow Transplantation, 259 W. Campus Drive, CCSR, Stanford, CA. 94305-5623.
E-mail address: AntoniaMaria.Mueller@usz.ch (A.M.S. Müller).

https://doi.org/10.1016/j.bbmt.2019.08.001
1083-8791/

patients appear to benefit but most do not, confirming that cGVHD is not one distinct disease entity but the end stage of various chronic inflammatory processes yet to be deciphered in detail. One factor that has limited our understanding of the pathophysiology of cGVHD is the lack of representative preclinical models.

Models for aGVHD commonly use transplants from parent into F1 offsprings or fully MHC-mismatched donor–recipient pairs. In general, these models result in a fulminant, aggressive clinical syndrome characterized by diarrhea, weight loss, and high mortality. Fewer models use MHC-matched strain combinations that have genetic disparity in minor histocompatibility antigens (miHAs) [12,13]. Many of these do not display manifestations of aGVHD or cGVHD, and therefore attempts to model a more protracted disease with less inflammatory but more fibrotic changes have been challenging.

A common model used to study cGVHD is the MHC-matched B10.D2 into BALB/c combination, which gives transient signs of skin GVHD around day +40 to +50 [14-16]. Also frequently used is the MHC-mismatched C57BL/6 into B10.BR model in which aberrant germinal center formation results in pathologic IgG-antibody deposition in the lung and a murine form of bronchiolitis obliterans [17]. Although these combinations replicate certain features of cGVHD, a protracted time course with multiorgan involvement homologous to human cGVHD is not observed.

Here we studied several MHC-matched, miHA-mismatched strain combinations over an extended time period to assess signs of aGVHD and cGVHD. The most representative model resulted from transplants of C57BL/6 (B6) grafts into BALB.B mice in which recipients developed aGVHD that gradually transitioned into a syndrome of cGVHD. aGVHD with ruffled fur, diarrhea, weight loss, and T cell dose-dependent lethality was first described in this strain combination by Korngold et al. in 1990 [18]. We previously reported in this model that alloreactive T cells acutely impair hematopoietic recovery and immune function post-HCT, indicating that bone marrow (BM) and lymphoid organs are major aGVHD targets [19,20]. Here, we studied the long-term effects of such transplants and found that the early disruption of marrow and lymphoid tissues is followed by a clinical syndrome that accurately simulates the pleomorphic disease of human cGVHD.

METHODS

Mice

The following strain combinations were studied. C57BL/6 mice ($H2^b$) were donors for BALB.B recipients ($H2^b$) and vice versa. B10.D2 mice ($H2^d$) were donors for BALB/c recipients ($H2^d$). BALB.K mice ($H2^k$) received grafts from AKR/J ($H2^k$) donors. AKR/B ($H2^b$) mice were donors for C57BL/6 ($H2^b$) mice and vice versa. AKR/B ($H2^b$) mice were donors for BALB.B mice ($H2^b$). All animal studies and protocols were approved by the Institutional Administrative Panel on Laboratory Animal Care of Stanford University.

Hematopoietic Stem Cell Transplantation

Recipient mice underwent myeloablative total body irradiation and were infused with a radioprotective dose of fluorescent activated cell sorter (FACS)-purified KTLS-hematopoietic stem cell (HSC) (c-KIT + Thy1.1^{low}, Lin^{neg}, Sca-1 + Lin^{neg}) alone or supplemented with titrated numbers of whole splenocytes ($1 \times 10^{5-8} \times 10^7$) or isolated T cell subsets.

Cell Harvest and Flow Cytometry

Cell suspensions from BM and spleens and infiltrating cells from liver and intestines were stained using standard protocols. For measurement of intracellular IL-17A and IFN-γ expression cell suspensions were stimulated with phorbol myristate acetate (PMA), ionomycin, and monensin for 5 hours at 37°C before staining.

Immunohistochemistry

Thymic sections were stained with anti–mouse keratin 5, anti–keratin 8, and biotin-AIRE. FITC-donkey anti–rat IgG, Cy5-donkey anti–rabbit IgG, and streptavidin-alexa fluor 350 were used as secondary antibodies.

RESULTS

Severity of GVHD Differs Among MHC-Matched, miHA-Mismatched Strain Combinations

Recipient BALB.B, BALB.K, BALB/c, C57BL/6 (B6), and AKR/b mice (male and female) were lethally irradiated and received 2000 to 3000 KTLS-HSC with or without titrated numbers of lymphocytes from miHA-mismatched female donors. In total, 7 different strain combinations were studied. Across all strains, transplantation of pure HSCs was associated with 100% survival and no signs of GVHD. Grafts supplemented with T cells, given within whole splenocytes, induced early GVHD (before day +50 post-HCT) in the following strain combinations: B6 into BALB.B ($H2^b$; Figure 1A,B), B10.D2 into BALB/c ($H2^d$; Figure 1C,D), and AKR/J into BALB.K ($H2^k$; Figure 1E,F). Clinical manifestations of GVHD and severity of symptoms differed by strain combination despite the identical genetic background of all 3 recipients (see below). At a graft splenocyte dose of 1×10^7 no clinical evidence of aGVHD or cGVHD within 200 days post-HCT was observed in transplants of BALB/B into B6 ($H2^b$), AKR/B into BALB.B ($H2^b$), AKR/B into B6 ($H2^b$), and B6 into AKR/B (Figure 1G,H).

aGVHD Transitions to cGVHD in the B6 into BALB.B Model

BALB.B recipients of B6 grafts composed of HSCs plus splenocytes at doses of 1×10^6 and 1×10^7 developed aGVHD with a mortality of 22% and 33% by day +50, respectively. CD4$^+$ cells had the full potency to induce lethal GVHD, whereas CD8$^+$ cells resulted in no lethality (Figure 2A). Weight loss was a hallmark of aGVHD (Figure 2B). Mice receiving only purified HSCs developed no GVHD; hence, this group served as controls in all studies. Recipients of HSCs plus CD8$^+$ cells also recovered and demonstrated stabilization of weight soon after transplant and displayed no other signs of GVHD. In contrast, in mice given HSCs plus splenocytes or CD4$^+$ cells, weight loss was more severe and persisted longer. Of note, male recipients of female grafts had more pronounced weight loss than female recipients of female grafts (Figure 2B). In addition to weight loss, clinical symptoms of aGVHD in these mice included diarrhea, swollen red eyes, hunched posture, and ruffled fur. Mice surviving aGVHD stabilized around day +40 to +50 post-HCT. After a period of clinical quiescence >50% of recipients of T cell–replete grafts gradually showed physical manifestations consistent with cGVHD beyond day +120 post-HCT. These manifestations included cloudy corneas, ruffled fur, hunched back posture, cutaneous excoriations at the pinna of the ears and tails, and, at very late time points, areas of alopecia on the trunk. In addition to those animals that showed overt cGVHD, a subgroup displayed subclinical signs, such as a runting syndrome manifested by smaller than normal size (Figure 1B).

Histologic analyses (hematoxylin and eosin) of the organs from the early phase post-HCT revealed a thickened intestinal wall and a dense, inflammatory infiltrate predominantly composed of small mature lymphocytes in the lamina propria and epithelium, consistent with the diagnosis of aGVHD. At time points beyond day +50 the mucosa recovered, and there were no histologic signs of cGVHD (Figure 2C). Livers of mice transplanted with grafts that contained splenocytes or CD4$^+$ cells displayed periportal inflammation with small mature-appearing lymphocytes during the early phase post-HCT. Over the course of many months the infiltrates worsened, showing extensive periportal infiltrates at 1 year post-HCT with disruption of the physiologic liver architecture (Figure 2D). As noted above, the pinna of the ears was affected in a subset of animals given grafts containing CD4$^+$ cells, and histology revealed severe inflammation characterized by parakeratosis and

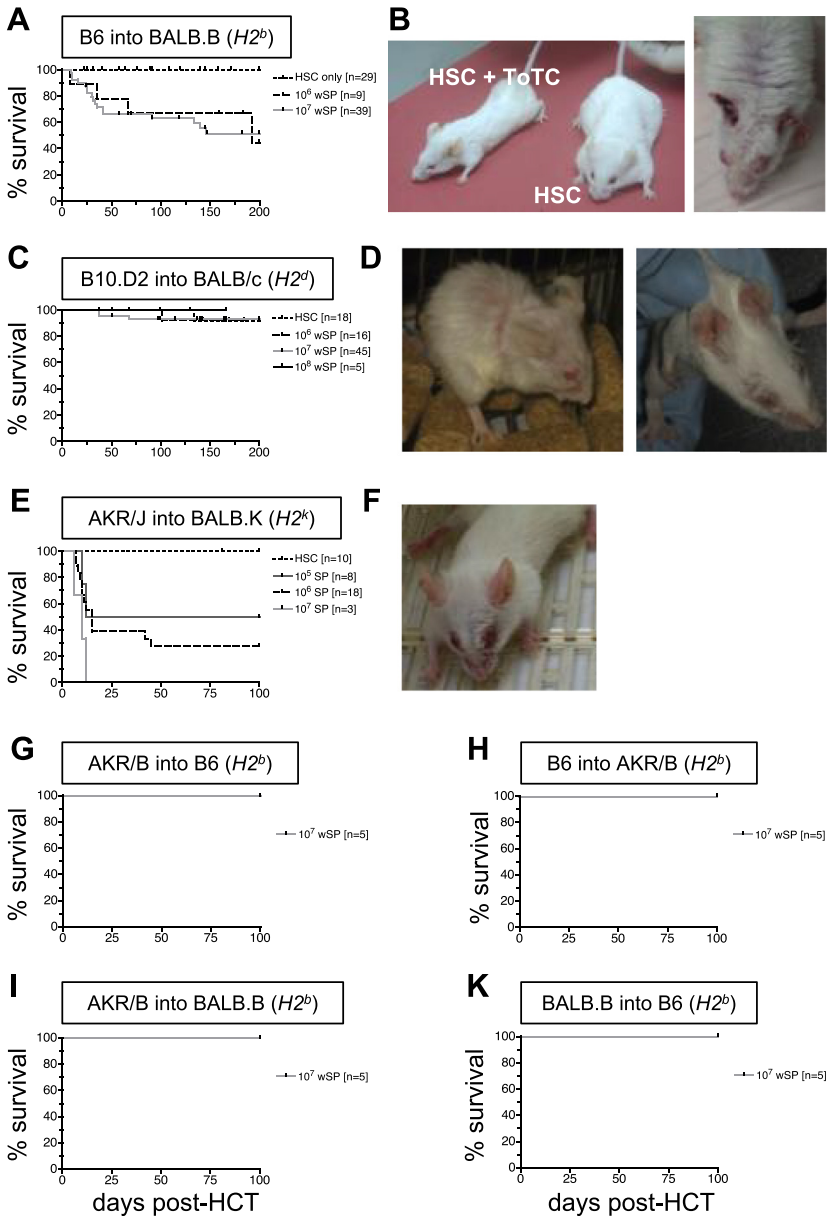

Figure 1. Kaplan-Meier curves displaying survival and clinical phenotype in MHC-matched, miHA-mismatched strain combinations. (A) Survival curves of C57/BL6 (B6) into BALB.B transplants. Recipient BALB.B mice received lethal (800 cGy) total body irradiation (TBI) and transplantation of grafts composed of 3000 KTLS-HSCs alone (n = 29) or in combination with 1×10^6 (n = 9) or 1×10^7 (n = 39) whole splenocytes (wSP). (B) Subclinical and clinical cGVHD in BALB.B recipients of B6 grafts at 1 year post-HCT. Left: Male mouse given HSC + T cells with subclinical GVHD ("runting") as compared with a recipient given HSCs alone. Right: HSC + T cell ($CD4^+$+$CD8^+$) recipient with manifestations of cGVHD of the skin, eyes, and overt wasting syndrome. (C) Survival curves of B10.D2 into BALB/c transplants. BALB.B recipients received lethal (800 cGy) TBI and transplant of grafts composed of 3000 KTLS-HSCs alone (n = 18) or in combination with 1×10^6 (n = 16), 1×10^7 (n = 45), or 1×10^8 (n = 5) wSP. (D) Clinical phenotype of early (between days 20 and 40) cGVHD in BALB/c recipients of B10.D2 HSC+wSP grafts demonstrating areas of alopecia on the back, inflammation of the skin of the ears, and conjunctivitis-like features. (E) Survival curves of AKR/J into BALB.K transplants. BALB.K recipients received 700 cGy TBI and transplant of grafts composed of 3000 KTLS-HSCs alone (n = 10) or in combination with 1×10^5 (n = 8), 1×10^6 (n = 18), or 1×10^7 (n = 3) wSP. (F) aGVHD with severe diarrhea, weight loss, and red eyes in BALB.K recipients of T cell–replete AKR/J grafts. (G-K) Survival curves of recipients of 3000 KTLS-HSCs + 1×10^7 wSP (n = 5) from specified donor strains. Recipients received lethal dose radiation. (G) AKR/B into B6 (950 cGy), (H) B6 into AKR/B (950 cGy), (I) AKR/B into BALB.B (800 cGy), and (K) BALB.B into B6 (950 cGy).

significant thickening of the dermis with architecture that was completely effaced by a dense inflammatory infiltrate. The adipose tissue was entirely replaced by a dense fibrotic infiltrate composed of fibroblasts and increased vascularization. Recipients of pure HSCs had an unremarkable histology of the skin (Figure 2E).

This spectrum of aGVHD transitioning into cGVHD best represented the human scenario; therefore, further studies focused on the B6 into BALB.B strain combination.

Ocular GVHD in the B6 into BALB.B Model

Clinically, ocular GVHD poses a major problem because inflammation in ocular tissues is one of the most frequent cGVHD manifestations. Beyond 6 months post-HCT many recipients of T cell–replete grafts acquired "cloudy" eyes. Corneal changes were histologically evaluated at 12 and 18 months (Figure 3A) using a scale ranging from 0 to 9 based on 4 parameters: thickness, presence of blood vessels, inflammatory cell infiltrates, and keratinization (Supplementary Table 1) [21,22].

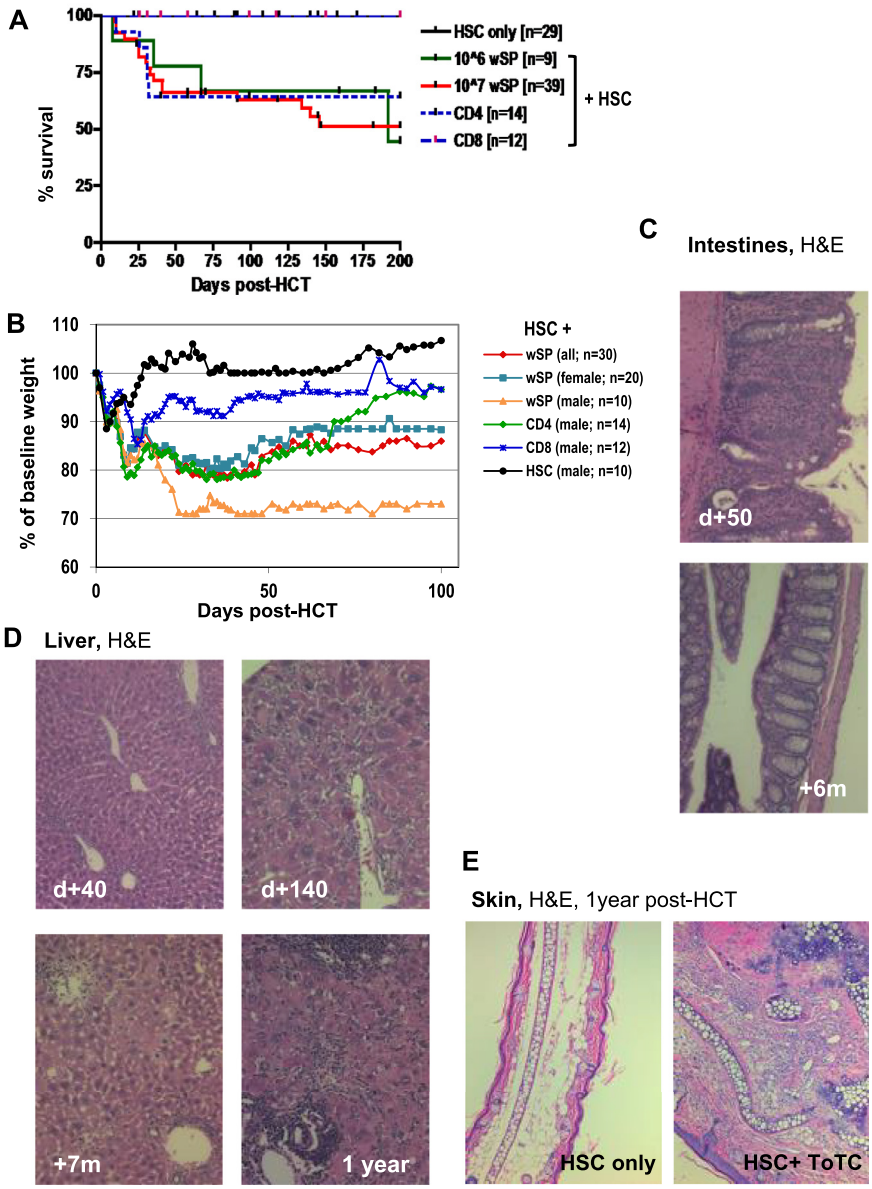

Figure 2. aGVHD and cGVHD in the B6 into BALB.B model. (A) Survival curves of lethally irradiated BALB.B recipients of B6 HSCs alone (n = 29, black line, 100% survival), HSC + 10^6 wSP (n = 9, green), HSC + 10^7 wSP (n = 39, red), HSC + 3 × 10^6 $CD4^+$ cells (n = 14, blue dotted), and HSC + 2 × 10^6 $CD8^+$ cells (n = 12; blue dotted line with red marks, 100% survival). (B) Weight loss, recorded as percent of baseline weight, in recipients of HSCs alone (n = 10, black); HSC + 1 × 10^7 wSP (n = 30, red), which were further separated into female recipients of female grafts (n = 20, light blue) and male recipients of female grafts (n = 10, yellow); male recipients of female HSC + $CD4^+$ cells (n = 14, green); and male recipients of HSC + $CD8^+$ cells (n = 12, dark blue). (C) H&E-stained sections of large intestine of representative mice with aGVHD at the indicated time points. At day +50 post-HCT the intestinal wall appeared thickened and the lamina propria and the epithelium infiltrated by a dense, inflammatory infiltrate predominantly composed of small mature lymphocytes with fewer neutrophils and plasma cells. At 6 months (+6m) post-HCT the large intestine appeared unremarkable without any residual inflammation. (D) H&E-stained liver sections at indicated time points post-HCT (day +40, day +140, +7 months, 1 year) at 10× magnification. Mice transplanted with HSCs + wSP developed periportal inflammation in the liver 40 days post-HCT that was predominantly composed of small mature-appearing lymphocytes. Over the course of a year the infiltrate worsened, showing extensive periportal infiltrates at 1 year after transplant. (E) H&E-stained skin sections of mice are shown 1 year post-HCT. Recipients of HSC + T cells ($CD4^+$+$CD8^+$) developed a severe inflammation in the skin of the ear characterized by parakeratosis and thickening of the dermis with completely effaced architecture and characterized by a dense inflammatory infiltrate of small mature lymphocytes, with fewer macrophages and neutrophils. The adipose tissue was entirely replaced by a dense fibrotic infiltrate composed of fibroblasts and increased vascularization. To the left, mice that had received HSCs only with unremarkable histology of the skin.

In contrast to mice receiving HSCs only, 12 of 13 animals given T cell–replete grafts had demonstrated corneal involvement. Recipients of $CD4^+$+$CD8^+$ cells exhibited higher corneal GVHD scores compared with recipients of $CD4^+$ or $CD8^+$ cells (scores of 7.25 ± 1.5 versus 4.5 ± .7 and 3.25 ± 2.75, respectively). Although all groups trended higher scores than HSCs alone, because of limited sample size, only the $CD4^+$+$CD8^+$ group reached statistical significance (1-way analysis of variance $P < .05$) (Figure 3B,C).

Naïve $CD4^+$ Cells Are Responsible for aGVHD in the B6 into BALB.B Model

Having observed in this strain combination the capacity of unfractionated splenic $CD4^+$ cells to induce GVHD, we examined the effects of adoptively co-transferred $CD4^+$ cell subsets. Naïve ($CD62L^+$ $CD44^-$) $CD4^+$ cells caused a severe and lethal aGVHD, even more severe than bulk $CD4^+$ cells, whereas mice given effector memory (EM) $CD4^+$ cells ($CD62L^-$ $CD44^+$) displayed no clinical signs of GVHD (Figure 4A,B). The BM is a

A

Graft	n (12m post-HCT)	n (18m post-HCT)
HSC only	2	2
HSC+CD4$^+$	2	0
HSC+CD8$^+$	2	2
HSC+ CD4$^+$+CD8$^+$	3	1
wSP	0	3

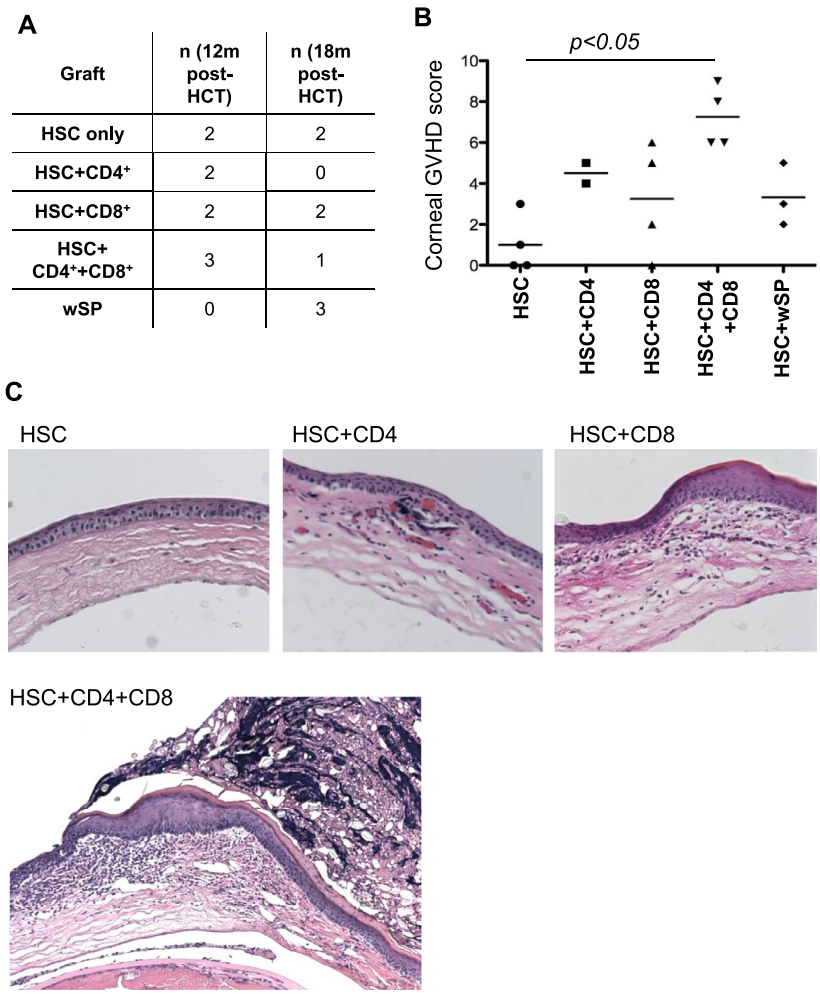

Figure 3. Ocular GVHD in the B6 into BALB.B model. (A) BALB.B recipients of B6 HSC only, HSC + 3 × 10^6 CD4$^+$, HSC + 2 × 10^6 CD8$^+$, or HSC + 3 × 10^6 CD4$^+$+2 × 10^6 CD8$^+$ cells were observed for 12 to 18 months post-HCT and then killed for histologic workup of the eyes. (B) Composite corneal GVHD score as determined by corneal thickness, corneal vessel immigration, presence of inflammatory cell infiltrates in the cornea, and hyperkeratinization for the transplanted groups. (C) Representative H&E-stained corneal histology recipients of pure HSC with no histologic abnormalities (top, left: 12 months post-HCT), HSC+CD4$^+$ (top, middle: 18 months post-HCT), HSC+CD8$^+$ (top, right: 18 months post-HCT), and HSC+CD4$^+$+CD8$^+$ (bottom, left: 12 months post-HCT).

major target organ of GVHD in this strain combination, resulting in severe suppression of B lymphopoiesis [19]. Here we show that naïve CD4$^+$ cells suppress the regeneration of the B-lymphoid lineage, whereas effector memory CD4$^+$ cells did not impact on prompt B cell recovery (Figure 4C). Of note, naïve CD4$^+$ cells contained higher proportions of regulatory T cells than effector memory CD4$^+$ cells, as determined by co-staining for FoxP3 (Supplementary Figure 1). There were no differences in the proportion of T cells in the blood of recipients of HSCs alone or HSCs + bulk CD4$^+$, naïve, or effector memory CD4$^+$ cells at 1 and 2 months post-HCT (Figure 4D). However, chimerism analysis of T cells at 1 month post-HCT revealed that in HSC recipients most blood T cells were host derived, whereas a smaller proportion of T cells originated from donor HSCs. In recipients of bulk CD4$^+$ or naïve CD4$^+$ cells most T cells in the blood were expanded adoptively co-transferred cells, whereas fewer T cells originated from either the donor HSCs or the residual host compartment. In contrast, in recipients of HSCs plus effector memory CD4$^+$ cells no co-transferred expanded T cells were detected, but most T cells were derived from donor HSCs in addition to some host T cells (Figure 4E).

The observation that no effector memory CD4$^+$ cells were present in the blood raised such questions as what is the fate of these co-transferred cells and is the lack of GVHD due to their nonpersistence? To address these questions, we performed comprehensive chimerism analyses on multiple tissues including blood, spleen, lymph nodes, BM, and liver on day +100 post-HCT from recipients of all graft types (HSCs alone, HSC + bulk CD4$^+$ cells, HSC + naïve CD4$^+$ cells, or HSC + effector memory CD4$^+$ cells). Figure 4F shows representative FACS plots displaying the origins of the T cells in these tissues for recipients of HSC plus effector memory CD4$^+$ cells. The findings from all graft groups from day +100 are shown in Supplementary Figure 2. At this time point in all groups, T cells originating from donor HSCs dominated blood, spleens and lymph nodes. However, distinct differences in T cell origin were noted in the BM and liver. The adoptively co-transferred CD4$^+$ cells of all subtypes were present in high numbers in these tissues, including the effector memory CD4$^+$ cells. In fact, the co-transferred bulk and naïve CD4$^+$ cells were the dominant T cell subpopulations in liver and BM (Figure 4F, Supplementary Figure 2). In recipients of co-transferred CD4$^+$ cells (regardless of the subset composition) the host-derived T cells were the smallest subset, whereas they were dominant in the BM and liver of HSC-only recipients. Taken together, these findings demonstrate co-transferred T cell subsets appear to home and persist for an extended period in

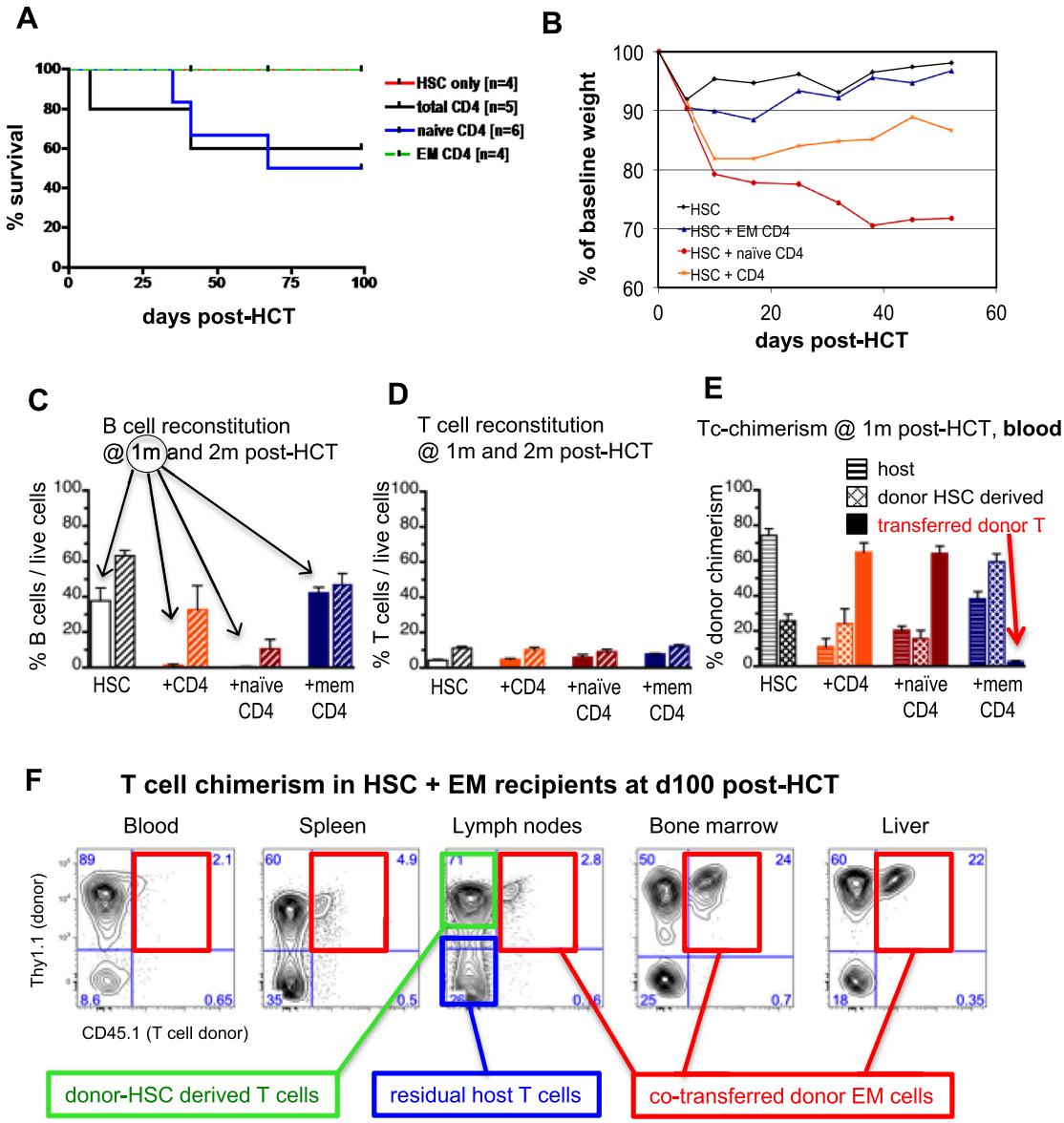

Figure 4. Naïve CD4$^+$ cells are responsible for aGVHD in the B6 into BALB.B model. Lethally irradiated BALB.B mice were transplanted with HSCs alone (n = 4) or HSC plus total CD4$^+$ cells (n = 5), naïve CD62L$^+$CD44$^-$CD4$^+$ cells (n = 6), or effector memory (EM) CD62L$^-$CD44$^+$CD4$^+$ cells (n = 4). HSCs were derived from Thy1.1$^+$CD45.2$^+$ donors, CD4$^+$ cells from Thy1.1$^+$ CD45.1$^+$ donors. (A) Survival curves of BALB.B recipients of CD4 subset grafts. (B) Weight loss with weights recorded as percent of baseline weight. (C) B cell reconstitution in the blood at 1 and 2 months post-HCT occurred promptly in recipients of HSCs alone or HSC + EM CD4$^+$, whereas recovery at 1 month was severely impaired in recipients of bulk CD4$^+$ and naïve CD4$^+$ cells. In recipients of naïve CD4$^+$ cells severe suppression of B lymphopoiesis was still noted at 2 months post-HCT. (D) Blood T cell recovery at 1 and 2 months post-HCT was slow in all transplant groups with no major differences between groups. (E) T cell chimerism in the blood at 1 month post-HCT revealed that in HSC recipients most T cells were residual host type. In recipients of HSCs plus bulk or naïve CD4$^+$ cells, a fraction of the T cell compartment were derived from residual host T cells, fewer were from newly generated T cells originating from the donor HSC, whereas most T cells were from expanded, adoptively co-transferred T cells. In recipients of HSC + EM CD4$^+$ cells, T cells comprised nascent, newly generated donor T cells and residual host T cells, whereas adoptively co-transferred T cells were not detectable in the blood. (F) T cell chimerism of blood, spleen, lymph nodes, BM, and liver of recipients of HSC + EM CD4$^+$ cells on day +100 post-HCT. Adoptively transferred donor EM cells were primarily found in the BM and liver, whereas only low levels were detected in blood and lymphoid organs.

variable tissues of recipients. Blood and even spleen may not be the optimal tissues to track the whereabouts of co-transferred cell populations. These findings are particularly relevant in the era of transferred therapeutic lymphocytes.

aGVHD Damages Thymic Cells Involved in T Cell Selection

As we and others have previously published, the thymus is a known target of aGVHD [20,23-25]. Here we observed after lethal irradiation and transplant of pure HSCs prompt recovery of the thymic tissue. Normal proportions of CD4/CD8 double negative, double positive (DP), CD4$^+$ single positive (SP), and CD8$^+$ SP populations were measured in thymic cell suspensions at 4 weeks post-transplant (Figure 5A). In contrast, the thymuses of recipients of HSCs + T cells had reduced proportions of CD4/CD8 DP cells and an increased proportion of CD4$^+$ SP and CD8$^+$ SP subpopulations (Figure 5B). Although DP cells largely originated from donor HSCs (CD45.2 GFP$^+$), SP cells were adoptively co-transferred donor T cells (CD45.1$^+$). The observation that co-transfer of mature donor T cells disturbed the process of thymic regeneration was also seen by immunofluorescence staining of thymic tissues. At day +58 post-HCT, recipients of HSC plus CD4$^+$ cells had lower proportions of

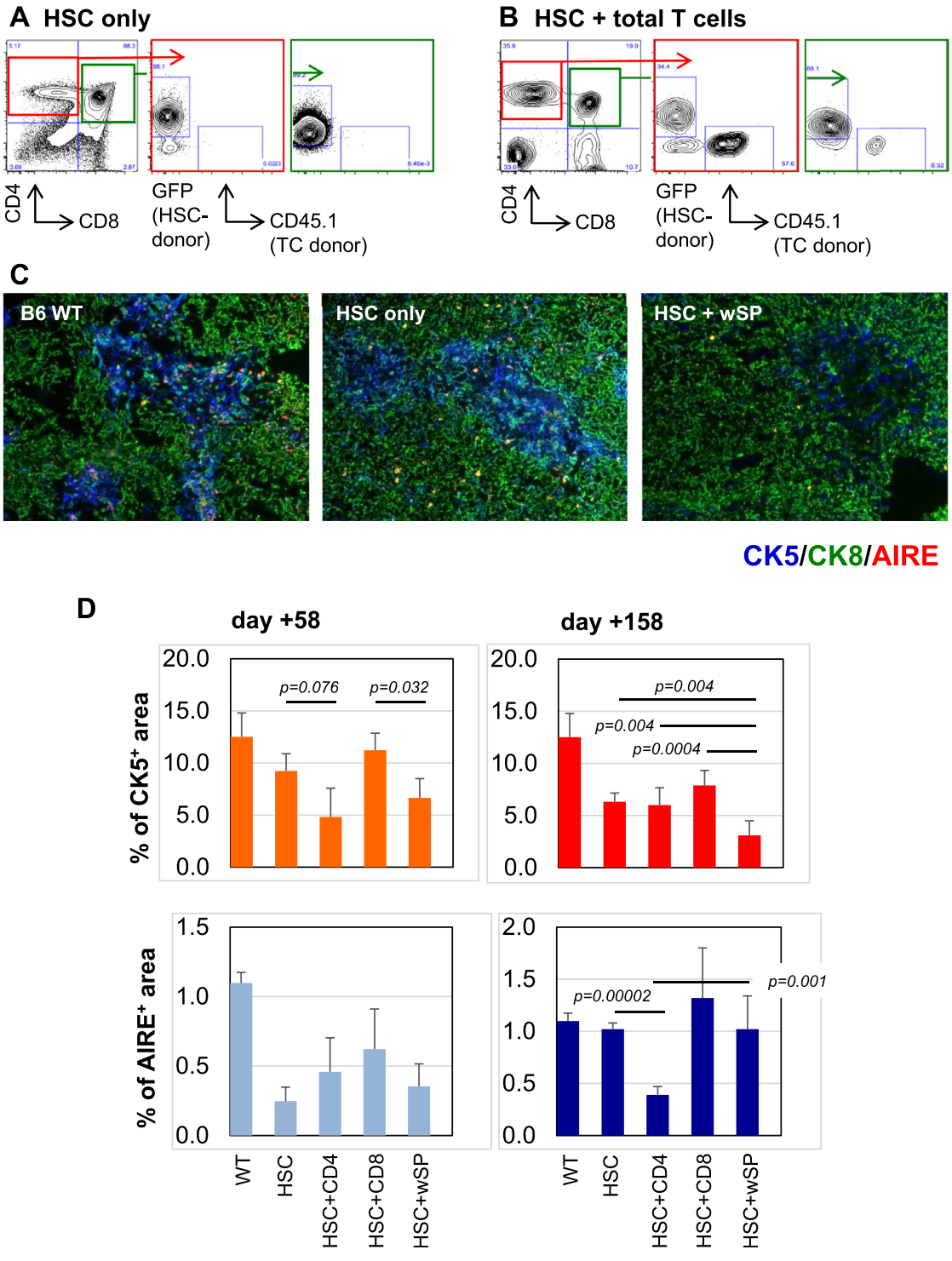

Figure 5. Thymic damage and reconstitution during and after aGVHD. Lethally irradiated BALB.B mice were transplanted with HSCs alone or HSC + $CD4^+$, HSC + $CD8^+$, or HSC + total T cells (TCs; $CD4^+$+$CD8^+$) or wSP. (A) Representative FACS plots of a thymus from a HSC-only recipient at 4 weeks post-HCT revealing normal proportions of CD4/CD8 double negative, DP, $CD4^+$SP, and $CD8^+$SP subpopulations (left plot). SP and DP populations originated from donor HSCs (GFP^+). (B) Representative FACS plots of a thymus from an HSC + TC recipient at 4 weeks post-HCT revealing reduced proportion of CD4/CD8 DP cells but an increased proportion of $CD4^+$ SP and $CD8^+$ SP subpopulations. Although DP cells largely originated from donor HSCs (CD45.2 GFP^+), SP cells were adoptively co-transferred donor T cells ($CD45.1^+$). (C) Immunofluorescence staining of thymic sections on day +158 post-HCT. Blue stains cytokeratin 5 that marks mTEC, green stains cytokeratin 8, and red stains AIRE. The left image shows a section of a thymus from an unmanipulated wild-type mouse. In the middle a section of a recipient of pure HSCs is shown. On the right side sections of an HSC + wSP recipient is shown. (D) Compiled data of percentages of the area positively stained for CK5 on day +58 (top, left) and day +158 (top, panel) and for AIRE on day +58 (bottom, left) and day +158 (bottom, right). Because of the similarity of the results the last 2 groups (total T cells and wSP) were combined. For each group 3 to 5 recipients were analyzed.

cytokeratin 5 positive ($CK5^+$) medullary thymic epithelial cells (mTEC) compared with recipients of pure HSCs or HSC plus $CD8^+$ cells (Figure 5C,D [top], Supplementary Figure 3). By day +158 it was recipients of HSCs plus splenocytes (1×10^7) that had the lowest proportion of mTECs compared with all other transplant groups (HSCs, HSC + $CD4^+$, HSC + $CD8^+$). Within the thymus mTECs provide a specialized microenvironment for survival, proliferation, and differentiation of immature T cells and are central to the education of nascent, donor-HSC derived, regenerating T cells. Damage inflicted to mTECs during aGVHD may therefore result in impaired negative selection with escape of autoreactive T cell clones into the periphery. In addition, donor grafts composed of HSC plus $CD4^+$ cells resulted in decreased expression of the autoimmune regulator AIRE in mTECS at day +158 post-HCT (Figure 5D [bottom]), further supporting the idea that GVHD can disturb negative selection of newly generated T cells and thereby give rise to "autoimmunity."

Th17 Cells Increase Over Time and Originate from Donor HSCs

Because IL-17 has emerged as a principal cytokine involved in autoimmunity, interest has been placed on Th17 cells as mediators of GVHD. Here, in the B6 into BALB.B model we studied emergence of IL-17^+CD4^+ Th17 cells in lymphoid and GVHD target organs at several time points post-HCT. Figure 6A,B shows FACS plots of lymph nodes at 1 year post-HCT from 2 representative recipients in each group that received either pure HSCs (Figure 6A) or HSC + T cells (Figure 6B). Figure 6 illustrates the variability in IL-17 and IFN-γ expression that differs substantially even between animals that received the same graft types. In some but not all animals IL-17 expressing $CD4^+$ cells co-expressed IFN-γ. Donor T cell infiltration of tissues (spleen, lymph nodes, liver, intestines) was high at 2 and 4 weeks post-HCT, but no measurable IL-17 production by $CD4^+$ cells was detected during this aGVHD phase (data not shown). Donor T cell infiltration decreased as aGVHD subsided in these tissues. In the receding T cell infiltrates beginning at >2 months post-HCT, $CD4^+$ IL-17^+ cells were detectable and their percentages within the $CD4^+$ cells increased slowly over time. As shown in Figure 6C, at all later time points (>2 months) post-HCT the relative levels of Th17 cells were higher in HCT recipients (of HSC ± T cells) compared with normal wild-type mice. However, there were no measurable differences in the levels between transplant groups (Figure 6A-C). Chimerism analysis of Th17 populations revealed that most Th17 cells originated from donor HSCs and were thus newly generated (Figure 6D, Supplementary Figure 4). Taken together, no correlation was observed between clinical manifestations of cGVHD and expression levels of IL-17.

GVHD in BALB Recipients Depends on Donor Type and MHC

Comparison of the 3 MHC-congenic strains of BALB mice used as recipients (BALB.B, $H2^b$; BALB/c, $H2^d$; BALB.K, $H2^k$) [26] revealed that despite their identical genetic background, the manifestations of GVHD varied substantially depending on donor background and allele type of the MHC-matched graft. B10.D2 into BALB/c is a commonly used model of cGVHD. Here, we show that lethality is minimal in recipients undergoing transplant of HSCs alone or HSCs plus high doses of T cells (up to 1×10^8 splenocytes) or T cell subsets (Figures 1C and 7A). BALB/c mice given T cell–containing grafts developed scattered skin lesions, primarily involving the pinna of the ears, and patches of alopecia between days +25 and +45 post-HCT (Figures 1D and 7B [bottom left]), whereas HSC-only recipients showed no abnormalities of the skin (Figure 7B [top left]). At around day +50 post-HCT skin lesions resolved spontaneously, and mice followed for >200 days did not develop recurrent or additional signs of cGVHD. Liver histology was normal at all time points throughout all experimental groups (Figure 7B [top and bottom right]), and animals recovered promptly from radiation-induced weight loss, whether or not the graft contained T cells (Figure 7C,D). Thus, in clean animal facility environments BALB/c recipients of B10.D2 allografts demonstrate transient skin lesions, low mortality, and no evidence of systemic GVHD.

BALB.K recipients of AKR/J grafts ($H2^k$) displayed a strikingly different clinical course. At a splenocyte dose of 1×10^7 all recipients died of fulminant aGVHD before day +20 post-HCT. To exclude the possibility that BALB.K mice are more susceptible to radiation, the dose was lowered to 700 cGy. Even with lower radiation and a 2-log lower dose of transplanted splenocytes (1×10^5), a 50% mortality due to GVHD was observed. The few sporadic survivors from these experiments did not developed signs of cGVHD. Only HSC recipients had 100% survival without signs of GVHD (Figures 1E,F and 7E). To investigate which role the inflammatory environment created by the conditioning plays in T cell activation, T cells were given as delayed donor lymphocyte infusions. All BALB.K mice who received their grafts of HSCs plus 1×10^7 AKR/J splenocytes on the day of radiation (day 0) died before day +10 post-HCT due to GVHD. Lethality among those given the same number of splenocytes 4, 7, and 10 days after the HSC transplant was lower with 50%, 80%, and 100% of survivors, respectively. Recipients of T cells and/or donor lymphocyte infusions on days 4 or 7 had high levels of donor T cell chimerism by 4 weeks post-HCT, consistent with a robust graft-versus-host immune cell effect that occurred in the permissive environment of these hosts immediately after transplant. In contrast, recipients of HSCs or HSCs + donor lymphocyte infusions on day 10 were mixed donor T cell chimeras (Supplementary Figure 5A). None of the mice in these latter groups developed cGVHD, consistent with their "tolerant" mixed chimeric state. Of note, although donor T cell chimerism was substantially higher in recipients of donor lymphocyte infusions on days 4 or 7, quantitative T cell levels were lower compared with the mixed chimeric recipients of HSCs only or HSCs plus donor lymphocyte infusions on day 10 (Supplementary Figure 5B). These data underscore the deleterious effect of T cells on immune recovery that is both quantitative and qualitative [19,20] and in its less overt form likely contributes to the immune dysregulation that leads to cGVHD.

DISCUSSION

The incidence of cGVHD continues to increase as transplants are given to older patients, more unrelated donors and mobilized peripheral blood rather than BM are used, and survival beyond the early post-transplant period improves. The limited understanding of the pathophysiology of cGVHD drives empiric treatments using drugs applied for aGVHD or which are supported more by theory than by proven pathophysiology. cGVHD is a complex and pleomorphic syndrome, and modeling in mice remains a challenge. Beyond the influence of genetic disparities, like humans, cGVHD in mice is influenced by environmental factors, such as hygiene standards of the animal facilities, nutrition, and so on. Hence, disparate experiences and observations are reported by different groups around the world.

Here, we carried out an in-depth approach to study mouse models of cGVHD, with the goal to identify those that most closely approximate human cGVHD, and to track the fate of

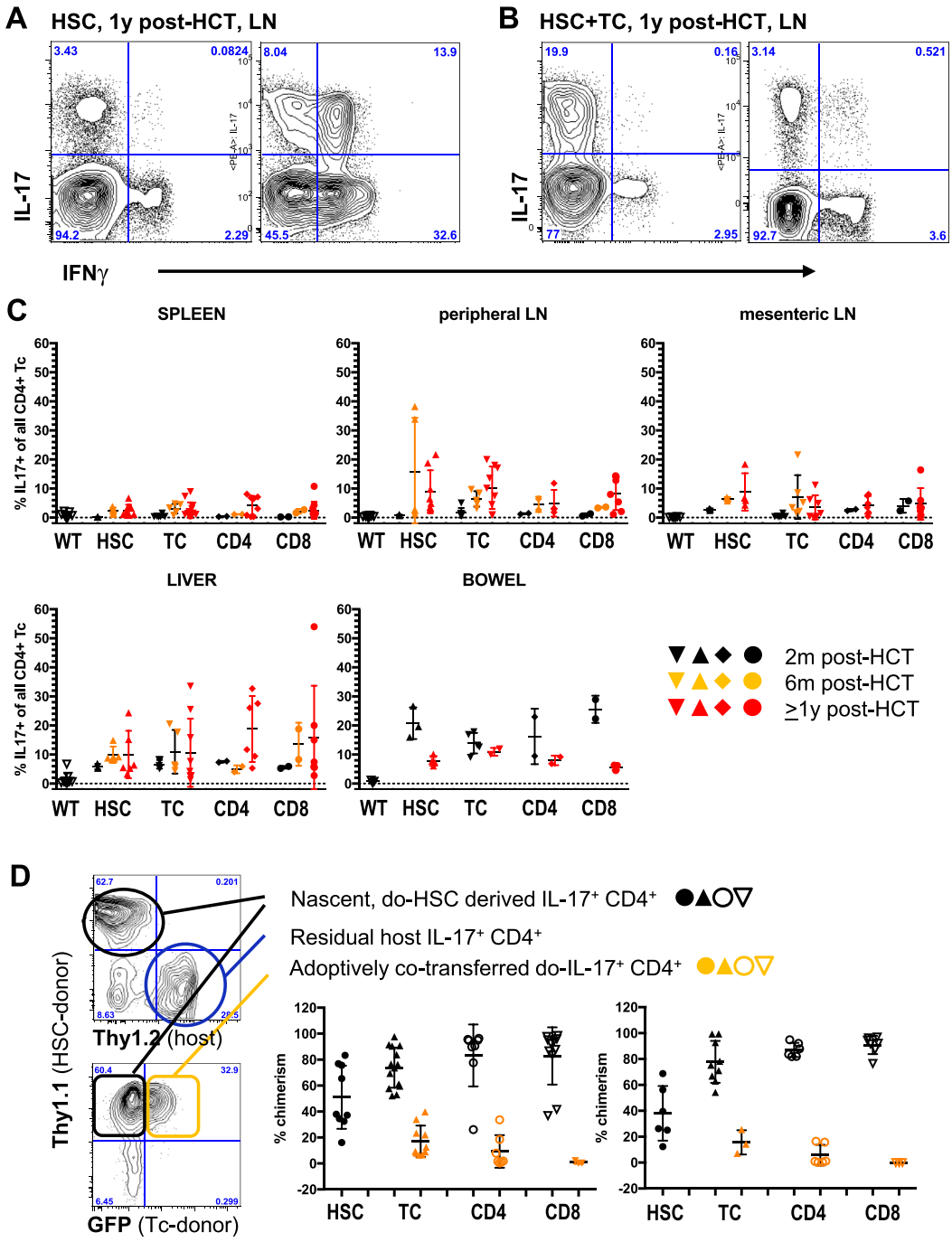

Figure 6. Emergence and chimerism of Th17. Lethally irradiated BALB.B mice were transplanted with HSCs alone or HSC + $CD4^+$ cells, HSC + $CD8^+$ cells, or HSC + total T cells (TC, $CD4^+$+$CD8^+$). (A and B) FACS plots of lymph nodes (LNs) from each 2 representative recipients of pure HSCs (A) or HSC + TC (B) at 1 year post-HCT. Parent plots were gated on $CD4^+$ cells. (C) Compiled FACS data displaying the percentage of IL-17 expressing cells within the $CD4^+$ T cell compartment in spleen, peripheral LN, mesenteric LN, liver, and the bowel. Shown are values obtained at 2 months (black), 6 months (yellow), and >12 months (red) post-HCT. (D) Left: Representative FACS plot demonstrating the gating strategy to assess chimerism in a recipient of HSC + TC. In this experiment HSC donors were Thy1.1 positive and could be distinguished from T cell donors, which expressed GFP and hosts (Thy1.2). Right: Compiled FACS chimerism data displaying the percentage (level of chimerism) of IL-17^+ $CD4^+$ cells originating from donor HSCs (black) versus expanded, co-transferred donor T cells (yellow).

contributing graft cell subsets. We focused on MHC-matched strains because the immunologic events of antigen presentation and T cell activation as well as the time required to accumulate the immunologic abnormalities are more homologous to human HCT compared with MHC-disparate mouse transplants. Seven MHC-matched, miHA-mismatched combinations underwent HCT of purified HSCs augmented with either whole splenocytes or selected T cell subsets. Only those combinations with recipients on the BALB background developed GVHD, whereas the reversal of donor–recipient pairs and other strain pairs studied did not develop signs of aGVHD or cGVHD, suggesting that BALB mice are more prone to perpetuation of aberrant immune responses. Furthermore, even though mice on the BALB background were prone to develop GVHD, the

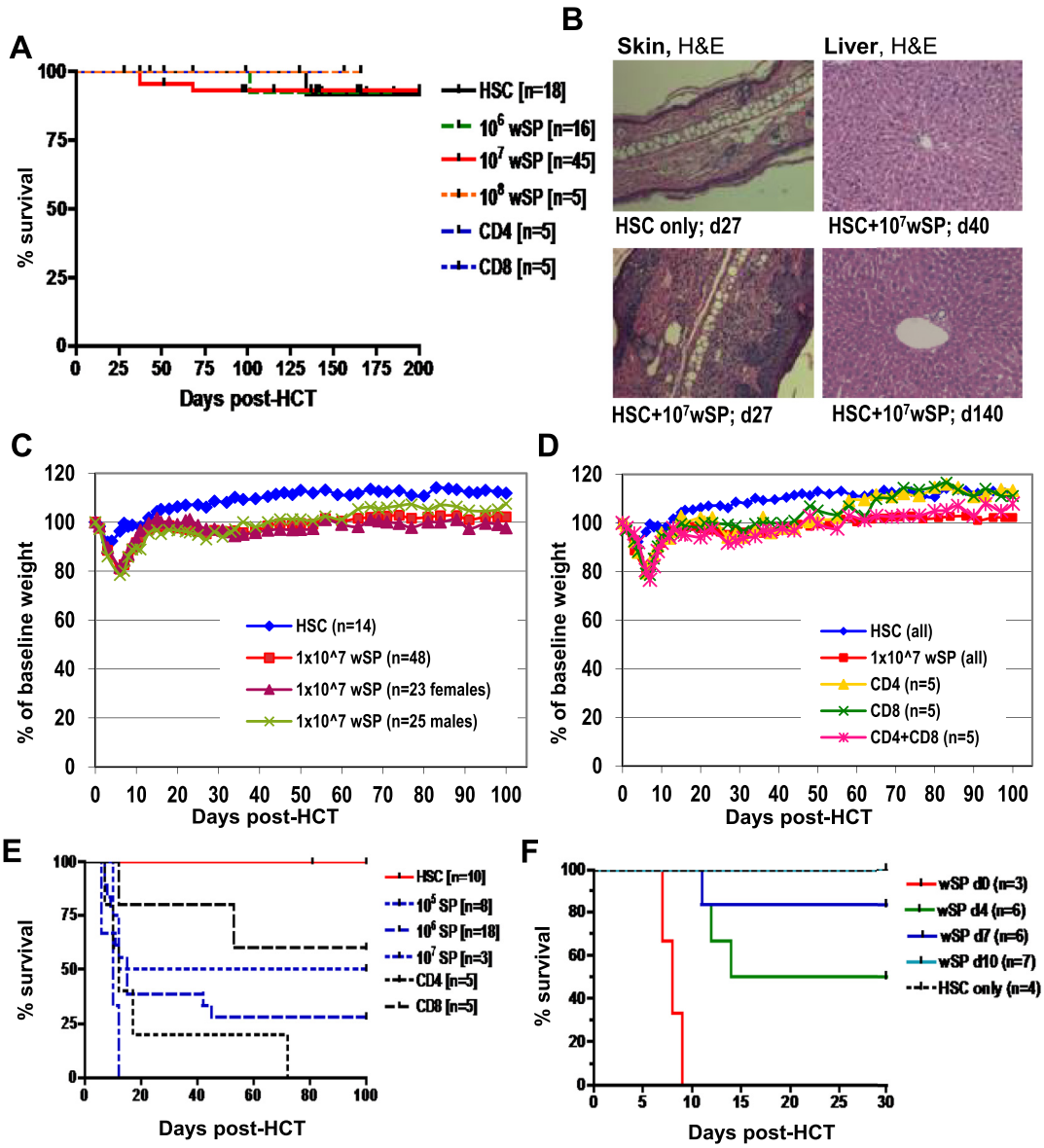

Figure 7. GVHD in BALB recipients depends on donor type and MHC. (A) Survival curves of lethally (800 cGy) irradiated BALB/c mice that were transplanted with B10.D2 HSCs alone (black) or HSCs in combination with 1×10^6 (green), 1×10^7 (red), or 1×10^8 (orange) wSP or HSCs + 4×10^6 $CD4^+$ cells or HSCs + 2×10^6 $CD8^+$ cells. (B) Top, left: Representative ear skin of mice 27 days post-HCT with HSCs demonstrating only a very mild inflammatory infiltrate with rare mononuclear cells. Bottom, left: Representative ear skin of mice 27 days after transplant with HSCs + 10^7 wSP demonstrating over 2-fold thickening of the skin with prominent parakeratosis and a dense inflammatory infiltrate composed of predominantly small lymphocytic cells. Of note, the adipose tissue is effaced and replaced by fibrosis and increased vascularization. Top and bottom, right: Representative sections of the liver of mice on day +40 and days +140 post-HCT with HSCs + 10^7 wSP demonstrated only minimal interstitial inflammatory infiltrate composed of predominantly lymphocytes which was cleared by days +140 post-HCT. Representative H&E stained sections of the skin and liver were taken at 10× magnification. (C) Weight loss (percent of baseline weight) in recipients of HSCs alone (blue, n = 14) or HSCs + 1×10^7 wSP (red, n = 48). The latter group was separated into female recipients of female grafts (pink, n = 23) and male recipients of female grafts (green, n = 25). There were no differences in weight course between groups. (D) Weight loss in recipients of HSCs alone (blue, n = 14), HSCs + 1×10^7 wSP (red, n = 48), HSCs + $CD4^+$ cells (yellow, n = 5), HSCs + $CD8^+$ cells (green; n = 5), and HSCs + $CD4^+$+$CD8^+$ cells (pink, n = 5). There were no differences in weight course between groups. (E) Survival curves of lethally irradiated (700 cGy) BALB.K mice that were transplanted with AKR/J HSC alone (red) or HSCs + 1×10^5 (n = 8), 1×10^6 (n = 18), or 1×10^7 (n = 3) wSP or HSCs + 4×10^5 $CD4^+$ cells (n = 5) or + 2×10^5 $CD8^+$ cells (n = 5). (F-H) Lethally irradiated (700 cGy) BALB.K mice were transplanted with HSCs alone (n = 4), HSCs + 1.5×10^7 wSP (n = 3) on day 0, or received HSCs on day 0 and 1.5×10^7 wSP on either day +4 (n = 6), day +7 (n = 6), or day +10 (n = 7) as donor lymphocyte infusions. (F) Survival curves.

clinical and histologic manifestations differed substantially depending on the donor strain and MHC allele type despite otherwise identical transplant conditions. This latter finding implies that different MHC types present different sets of minor antigens that make them differential targets for alloreactive attack, thereby influencing disease course, sites of organ involvement, severity of disease, and donor cell dose required to induce the disease.

Our data show for the first time that transplants of B6 into BALB.B mice provide an authentic model of cGVHD with a protracted time course and multiorgan involvement. In this model cGVHD is preceded by aGVHD, which is driven by adoptively transferred mature $CD4^+$ cells that acquire a Th1 phenotype. Lesions in the target organs evolve from inflammatory cells, which persist and gradually progress into fibrotic infiltrates with disruption of the tissue architecture. We previously

showed that the BM and lymph nodes are preferred targets of aGVHD, resulting in deleterious effects on hematopoiesis and immune function [19,20].

Here in this B6 into BALB.B model we further show several key findings. First, naïve $CD4^+$ cells had the strongest negative effect on hematopoietic reconstitution, particularly of the B cell lineage, and on GVHD manifestations, whereas effector memory $CD4^+$ cells neither induced overt GVHD nor impacted hematopoiesis. Both subsets contained $FoxP3^+$ regulatory T cells. Second, purified naïve and effector memory $CD4^+$ cells demonstrated different homing patterns and locations of persistence. Specifically, effector memory cells quickly egressed from the blood and were found long term in tissues such as BM and liver. This differential homing underscores the fact that examination of the blood only gives an incomplete picture of donor cell activities postinfusion, a concept of highest relevance in this era of cellular therapies. Third, the origins of the reconstituting T cell pool were linked to graft composition. Early post-HCT (1 month) in recipients of HSCs only most blood $CD4^+$ cells were host derived, and although at 3 months donor-derived HSCs dominated the blood and lymphoid tissues, the residual host T cells persisted and remained the predominant T cell source in the marrow and liver. In contrast, at 1 month post-HCT in recipients of bulk $CD4^+$ or naïve $CD4^+$ cells, most T cells in the blood were from these co-transferred cells and remained the predominant source in liver and BM at later time points, whereas HSC-derived donor cells comprised most $CD4^+$ cells in blood and lymphoid tissues. In recipients of HSC plus memory $CD4^+$ cells, at 1 month most reconstituting T cells were derived from donor HSCs, suggesting that donor memory cells may facilitate development of nascent T cells from donor HSCs. In these mice residual host T cells persisted in blood and lymphoid tissues in a similar fashion as in HSC-only recipients, further suggesting effector memory $CD4^+$ cells do not eradicate host T cells efficiently.

Fourth, in agreement with the findings by other groups [23-25,27], injury to the thymus by alloreactive T cells can result in impaired regeneration of essential thymic structures important in maintaining an appropriate T cell repertoire and lead to GVHD. In our model we note that mTECs, which are critical to negative T cell selection, are decreased in recipients of T cell–replete grafts compared with those given pure HSCs. In settings where mTECs are destroyed, autoreactive T cells can escape from the thymus into the periphery and contribute to cGVHD. We hypothesize that in this model it is damage to the thymus sustained during the acute phase and impaired thymic recovery that leads to multiorgan syndrome of cGVHD. Finally, we examined the role of IL-17 producing Th17 cells. Th17 cells have been widely implicated in the pathophysiology of autoimmune diseases; however, data regarding their relevance in the establishment of aGVHD and cGVHD are contradictory [7,28-35]. In our model aGVHD was driven by IFN-γ–producing $CD4^+$ cells, whereas IL-17–producing donor cells were undetectable early post-HCT. This observation suggests that in the presence of donor Th1 cells, development of Th17 cells is suppressed, as IFN-γ and T-bet produced by Th1 cells are known negative regulators of RORγT, the master regulator of Th17 [36]. Suppression of Th17 cells persisted beyond the acute phase: Recipients of T cell–replete grafts that survived aGVHD but later developed cGVHD did not demonstrate increased proportions of $CD4^+$ $IL\text{-}17^+$ cells. In some mice without overt aGVHD, $CD4^+$ $IL\text{-}17^+$ cells that originated primarily from donor HSCs were measurable beyond 2 to 6 months post-HCT. A clear correlation between IL-17 production and clinical phenotype was not observed, suggesting that in the B6 into BALB.B model, IL-17 is not a key driver of cGVHD. This finding is in line with data obtained in patients that have not supported a key role of IL-17 in GVHD induction [37].

In summary, our studies modeling cGVHD demonstrate that transplant of B6 into BALB.B mice is a highly viable model that mirrors the clinical and histologic scenarios of the human syndrome. This conclusion is based on the time course to disease development, clinical manifestations, and pathology that affect the eyes, liver, and skin, the most frequently affected tissues in cGVHD patients. This cGVHD syndrome is most likely caused by events early post-HCT, affecting BM [19] and thymus and thereby permitting breakdown of immune tolerance and the escape of autoreactive cells into the periphery within newly generated lymphocyte populations.

ACKNOWLEDGMENTS

The authors thank members of the Shizuru laboratories for helpful advice, critical discussion, and technical assistance.

Financial disclosure: Supported by the National Institutes of Health grants RO1 HL087240, PO1 HL075462, and PO1 CA049605 (to J.A.S.); the H.L. Snyder Medical Foundation (to J.A.S.); the Stinehart-Reed Foundation (to J.A.S.); the Virginia and D.K. Ludwig Fund for Cancer Research (to J.A.S.); the Gunn/Olivier Research Fund (to J.A.S.); and a postdoctoral fellowship training grant from the German Research Foundation (to A.M.S.M.).

Conflict of interest statement: There are no conflicts of interest to report.

Authorship statement: A.M.S.M. designed, performed and analyzed experiments, and wrote the manuscript. D.M. and S. H. performed and analyzed experiments. G.W. reviewed pathologies. M.F. and C.B. performed experiments. K.W., V.L.P., and R.B.L. gave critical advice and edited the manuscript. J.A.S. S designed experiments and wrote the manuscript.

SUPPLEMENTARY MATERIALS

Supplementary material associated with this article can be found in the online version at doi:10.1016/j.bbmt.2019.08.001.

REFERENCES

1. Filipovich AH, Weisdorf D, Pavletic S, et al. National Institutes of Health consensus development project on criteria for clinical trials in chronic graft-versus-host disease. I. Diagnosis and Staging Working Group report. *Biol Blood Marrow Transplant*. 2005;11:945–956.
2. Jagasia MH, Greinix HT, Arora M, et al. National Institutes of Health consensus development project on criteria for clinical trials in chronic graft-versus-host disease. I. The 2014 Diagnosis and Staging Working Group report. *Biol Blood Marrow Transplant*. 2015;21:389–401.
3. Ferrara JL, Deeg HJ. Graft-versus-host disease. *N Engl J Med*. 1991;324:667–674.
4. Horwitz ME, Sullivan KM. Chronic graft-versus-host disease. *Blood Rev*. 2006;20:15–27.
5. Lee SJ, Flowers ME. Recognizing and managing chronic graft-versus-host disease. *Hematol Am Soc Hematol Educ Progr*. 2008 (1):134–141.
6. Lee SJ, Vogelsang G, Flowers ME. Chronic graft-versus-host disease. *Biol Blood Marrow Transplant*. 2003;9:215–233.
7. Walter EC, Orozco-Levi M, Ramirez-Sarmiento A, et al. Lung function and long-term complications after allogeneic hematopoietic cell transplant. *Biol Blood Marrow Transplant*. 2010;16:53–61.
8. Flynn R, Paz K, Du J, et al. Targeted rho-associated kinase 2 inhibition suppresses murine and human chronic GVHD through a Stat3-dependent mechanism. *Blood*. 2016;127:2144–2154.
9. Yoon HK, Lim JY, Kim TJ, Cho CS, Min CK. Effects of pravastatin on murine chronic graft-versus-host disease. *Transplantation*. 2010;90:853–860.
10. Kim J, Choi WS, La S, et al. Stimulation with 4-1BB (CD137) inhibits chronic graft-versus-host disease by inducing activation-induced cell death of donor CD4+ T cells. *Blood*. 2005;105:2206–2213.
11. Nishimori H, Maeda Y, Teshima T, et al. Synthetic retinoid Am80 ameliorates chronic graft-versus-host disease by down-regulating Th1 and Th17. *Blood*. 2012;119:285–295.
12. Zeiser R, Blazar BR. Preclinical models of acute and chronic graft-versus-host disease: how predictive are they for a successful clinical translation. *Blood*. 2016;127:3117–3126.

13. Zeiser R, Blazar BR. Acute graft-versus-host disease—biologic process, prevention, and therapy. *N Engl J Med*. 2017;377:2167–2179.
14. Anderson BE, McNiff JM, Matte C, Athanasiadis I, Shlomchik WD, Shlomchik MJ. Recipient CD4+ T cells that survive irradiation regulate chronic graft-versus-host disease. *Blood*. 2004;104:1565–1573.
15. Claman HN, Jaffee BD, Huff JC, Clark RA. Chronic graft-versus-host disease as a model for scleroderma. II. Mast cell depletion with deposition of immunoglobulins in the skin and fibrosis. *Cell Immunol*. 1985;94:73–84.
16. Jaffee BD, Claman HN. Chronic graft-versus-host disease (GVHD) as a model for scleroderma. I. Description of model systems. *Cell Immunol*. 1983;77:1–12.
17. Srinivasan M, Flynn R, Price A, et al. Donor B-cell alloantibody deposition and germinal center formation are required for the development of murine chronic GVHD and bronchiolitis obliterans. *Blood*. 2012;119:1570–1580.
18. Korngold R, Wettstein PJ. Immunodominance in the graft-vs-host disease T cell response to minor histocompatibility antigens. *J Immunol*. 1990;145:4079–4088.
19. Muller AM, Linderman JA, Florek M, Miklos D, Shizuru JA. Allogeneic T cells impair engraftment and hematopoiesis after stem cell transplantation. *Proc Natl Acad Sci USA*. 2010;107:14721–14726.
20. Muller AM, Shashidhar S, Kupper NJ, et al. Co-transplantation of pure blood stem cells with antigen-specific but not bulk T cells augments functional immunity. *Proc Natl Acad Sci USA*. 2012;109:5820–5825.
21. Herretes S, Ross DB, Duffort S, et al. Recruitment of donor T cells to the eyes during ocular GVHD in recipients of MHC-matched allogeneic hematopoietic stem cell transplants. *Invest Ophthalmol Vis Sci*. 2015;56:2348–2357.
22. Perez VL, Barsam A, Duffort S, et al. Novel scoring criteria for the evaluation of ocular graft-versus-host disease in a preclinical allogeneic hematopoietic stem cell transplantation animal model. *Biol Blood Marrow Transplant*. 2016;22:1765–1772.
23. Teshima T, Reddy P, Liu C, Williams D, Cooke KR, Ferrara JL. Impaired thymic negative selection causes autoimmune graft-versus-host disease. *Blood*. 2003;102:429–435.
24. van den Brink MR, Moore E, Ferrara JL, Burakoff SJ. Graft-versus-host-disease-associated thymic damage results in the appearance of T cell clones with anti-host reactivity. *Transplantation*. 2000;69:446–449.
25. Wu T, Young JS, Johnston H, et al. Thymic damage, impaired negative selection, and development of chronic graft-versus-host disease caused by donor CD4+ and CD8+ T cells. *J Immunol*. 2013;191:488–499.
26. Cao TM, Lo B, Ranheim EA, Grumet FC, Shizuru JA. Variable hematopoietic graft rejection and graft-versus-host disease in MHC-matched strains of mice. *Proc Natl Acad Sci USA*. 2003;100:11571–11576.
27. Zhang Y, Hexner E, Frank D, Emerson SG. CD4+ T cells generated de novo from donor hemopoietic stem cells mediate the evolution from acute to chronic graft-versus-host disease. *J Immunol*. 2007;179:3305–3314.
28. Kappel LW, Goldberg GL, King CG, et al. IL-17 contributes to CD4-mediated graft-versus-host disease. *Blood*. 2009;113:945–952.
29. Carlson MJ, West ML, Coghill JM, Panoskaltsis-Mortari A, Blazar BR, Serody JS. In vitro-differentiated TH17 cells mediate lethal acute graft-versus-host disease with severe cutaneous and pulmonary pathologic manifestations. *Blood*. 2009;113:1365–1374.
30. Hill GR, Olver SD, Kuns RD, et al. Stem cell mobilization with G-CSF induces type 17 differentiation and promotes scleroderma. *Blood*. 2010;116:819–828.
31. Gartlan KH, Markey KA, Varelias A, et al. Tc17 cells are a proinflammatory, plastic lineage of pathogenic CD8+ T cells that induce GVHD without antileukemic effects. *Blood*. 2015;126:1609–1620.
32. Gartlan KH, Varelias A, Koyama M, et al. Th17 plasticity and transition toward a pathogenic cytokine signature are regulated by cyclosporine after allogeneic SCT. *Blood Adv*. 2017;1:341–351.
33. Chen X, Vodanovic-Jankovic S, Johnson B, Keller M, Komorowski R, Drobyski WR. Absence of regulatory T-cell control of TH1 and TH17 cells is responsible for the autoimmune-mediated pathology in chronic graft-versus-host disease. *Blood*. 2007;110:3804–3813.
34. Chen X, Das R, Komorowski R, van Snick J, Uyttenhove C, Drobyski WR. Interleukin 17 is not required for autoimmune-mediated pathologic damage during chronic graft-versus-host disease. *Biol Blood Marrow Transplant*. 2010;16:123–128.
35. Zhao D, Zhang C, Yi T, et al. In vivo-activated CD103+CD4+ regulatory T cells ameliorate ongoing chronic graft-versus-host disease. *Blood*. 2008;112:2129–2138.
36. Harrington LE, Hatton RD, Mangan PR, et al. Interleukin 17-producing CD4+ effector T cells develop via a lineage distinct from the T helper type 1 and 2 lineages. *Nat Immunol*. 2005;6:1123–1132.
37. Broady R, Yu J, Chow V, et al. Cutaneous GVHD is associated with the expansion of tissue-localized Th1 and not Th17 cells. *Blood*. 2010;116:5748–5751.